The Simulated Structure of Neutron Stars

Enrico Zammit Lonardelli

Student ID 9910821

Charles Smith

Student ID 9963262

ABSTRACT

Neutron stars were simulated by using the principle of hydrostatic equilibrium with Newtonian and General Relativistic gravitational models. The star was 'built' using numerical methods such as the Runge-Kutta 4th order method, with both an ideal non-interacting Fermi gas and soft-core interacting equation of states. Radius and mass dependence on the equation of state used was investigated as well as the density structure of the stars for comparison against observations. Using the Tolman-Oppenheimer-Volkov equation, with Bethe & Johnson's equation of state, the maximum mass of a neutron star was found to be (1.78840 ± 0.00004) solar masses with radius (9.262 ± 0.002) km and the maximum radius was found to be (11.156 ± 0.002) km with mass (0.98280 ± 0.00004) solar masses.

INTRODUCTION

'It doesn't matter how beautiful your theory is, it doesn't matter how smart you are. If it doesn't agree with experiment, it's wrong'-Richard P. Feynman. Neutron stars are perhaps the only loophole in today's physics to this argument, we cannot experimentally validate the structure of a neutron stars. Observations are used to develop theory and an equation of states. In this report neutron stars were simulated using numerical integration, the principle of hydrostatic equilibrium and two equations of state. The theorized matter distribution of compact stellar objects was stated before examining the method of 'building ' the star. We then aimed to show which of the equation of states tested best suits observation and why. Additionally, special relativistic rotation was added as a fictitious force to give understanding of rotational effects.

THEORY

STELLAR PROCESSES

If there was no opposing force to gravity, then there would only be gravitational singularities within the universe. Luckily in our universe there tends to be an opposition to gravity in the form of kinetic effects such as radiation pressure due to the hydrogen and helium fusion process in main sequence stars, angular momentum (centrifugal) effects or magnetic/ nuclear forces[q]. For white dwarves and neutron stars gravitational opposition is due to the Pauli exclusion principle which states that no two fermions may inhabit the same spacial co-ordinates. There is a distribution of non-zero momentum for fermions at 0 kelvin (cold matter), theoretically described by 'k space' [k].

After a star can no longer sustain nuclear fusion and dissipates all other free energies opposing gravitational contraction on its own mass, it collapses onto its core. If the collapse is violent then much of the core mass may be expelled by the rebound of such a process. The core if less than 1.4 solar masses M_s, Fermi pressure in the form of electron degeneracy will oppose gravitation and a white dwarf star is born[c]. If the stellar core is more massive than the Chandrasekhar limit of 1.4M_s, the electron degeneracy pressure will not stop the star from further collapse. Baryonic fermi degeneracy will support the star from collapse; This is a neutron star. If the core is more than approximately three solar masses a black hole is formed[c].

THE THEORETICAL STRUCTURE

The structure of nuclear matter with varying density from its crust into its centre is fundamental to comparing observation to simulation. So, we formed a theoretical spherically symmetrical density distribution based on current Standard Model of particle physics for our neutron star model.

On the surface/outer crust for densities less than $4.3x10^{14}kgm^{-3}$ a coulomb lattice structure of neutron rich nuclei is formed, due to inverse beta decay from the relativistic degenerate electrons. The nuclear binding energy peak representing the most stable nuclei will be slightly skewed by this effect. Beyond $4.3x10^{14}kgm^{-3}$ the inverse beta decay process becomes more prominent, causing the 'neutron drip', a process in which the neutron rich nuclei expel the neutrons into a neutron gas. Here, free electrons and neutrons co-exist in an equilibrium of superfluid gas. The neutron and electron gas with neutron rich nuclei can exist in this state up until the nuclear density of $2.3x10^{17}kgm^{-3}$. Interactions are very important between particles at densities above $2.3x10^{17}kgm^{-3}$. Passed the nuclear density, the nuclei begin to merge, in a process called nuclear saturation, causing complex inter-nucleon interactions. This gives rise to a superfluid of electrons, neutrons and protons where baryonic/neutron degeneracy exerts an outward pressure due to the Pauli exclusion principle. At densities of the order $1x10^{18}kgm^{-3}$ the pressure may cause pion condensation; Passed this density, in extremely dense cores quark matter is hypothesised to be formed[a][b][m].

BUILDING A STAR

For a star not to collapse or explode each infinitesimally thin spherical shell of the neutron star matter must be in an equilibrium of pressures. The balance must be between the outward pressure caused by the degeneracy of the matter and the gravitational forces inward due to the mass inside that shell; This is the principle of hydrostatic equilibrium[r].

Using the Newtonian gravitational model, the pressure gradient and therefore condition for stellar equilibrium at radius r due to gravity is

$$\frac{dP}{dr} = \frac{-Gm(r)\rho(r)}{r^2} \qquad (1).$$

where $\rho(r)$is the density of matter at r, G is the universal gravitation constant of gravitation and P is the pressure. The mass enclosed by a sphere of radius r ,$m(r)$ is given by the differential equation [r]

$$\frac{dm}{dr} = 4\pi r^2\rho(r) \qquad (2).$$

In Einstein's theory of gravitation, the corresponding condition for hydrostatic equilibrium is

$$\frac{dP}{dr} = \frac{-Gm(r)}{r^2}\frac{\left(1+\frac{P(r)}{\rho(r)c}\right)\left(1+4\pi r^3\frac{P(r)}{m(r)c}\right)}{\left(1-\frac{2Gm(r)}{rc^2}\right)} \qquad (3).$$

Equation (3)[m] is called the Tolman–Oppenheimer–Volkoff equation (TOV). The TOV shows explicit pressure dependence on the pressure gradient leading to greater gravitational forces at a smaller mass than equation (1). Equation (3) was predicted by Oppenheimer and Volkoff in 1939 using a cold Fermi gas (one very similar to our non-interacting model in the following section). They found a maximum neutron star mass of 0.7 $M_s$using the TOV[h].

The above equations have been used with numerical integration and equations of state (EOS) to model neutron stars. We compare the solutions of equations (1) and (3) and corresponding EOS's with observation.

THE EQUATION OF STATE

The equation of state describes the pressure and mass densities. In our models for simulations of neutron stars two equations of state were used, the Bethe-Johnson (BJ) and an ideal neutron gas EOS.

The Bethe Johnson EOS [d] is a modified Reid soft core interaction model, using neutron-neutron (N-N) potentials to produce a repulsive core via meson exchange[b]. The BJ EOS uses Yukawa functions with parameters set to model experimental N-N scattering data [b]. The BJ EOS is

$$P(n) = 363.44n^{2.54} \tag{4.a}$$

$$\rho(n) = 236n^{2.54} + nm_n \tag{4.b}$$

, where n is the number density of neutrons, $P(n)$ is the pressure in $MeVc^{-2}fm^{-3}$and $\rho(n)$ is the density in $MeVc^{-2}fm^{-3}$. A conversion factor to SI units was applied to equation (4) before application in the computational section. The BJ EOS is valid for the central density range of $(1.7 \times 10^{17} \leq \rho \leq 3.2 \times 10^{19})kgm^{-3}$ [b].

The ideal neutron gas EOS (NI) is the simplest model that can be used [a]. It is based on a non-interacting Fermi gas of neutrons. There are two parts to this equation of state; In the nonrelativistic regime the EOS is

$$P = \frac{\hbar}{5m_n^{\frac{8}{3}}}(3\pi^2)^{\frac{2}{3}}\rho^{\frac{5}{3}} \tag{.5.a}$$

The second part of the NI EOS in the relativistic approximation is given by

$$P = \frac{1}{3}\hbar c m_n^{\frac{-4}{3}}(3\pi^2)^{\frac{1}{3}}\rho^{\frac{4}{3}} \tag{.5.b}$$

The NI EOS is valid for $(0 \leq \rho \leq \infty)kgm^{-3}$[b], with the advised upper bound to be $(\rho \leq 5 \times 10^{17})kgm^{-3}$ due to the softening of the EOS relations due to N-N interactions. There is a critical density of value $\rho_c = 5 \times 10^{17}kgm^{-3}$ [j] specified for computational processes that acts as a bound between equations (5.a) and (5.b). The value ρ_c is derived as an approximate figure using

$$\varepsilon_F = \frac{\hbar^2}{2m_n}\left(3\pi^2\frac{N}{V}\right)^{\frac{2}{3}} \ll E_{mn} \tag{6}$$

[k], where ε_F is the Fermi energy of the neutron in this case, $\frac{N}{V}$ is the density of neutrons per unit volume in k space and E_{mn} is the rest mass of a neutron in joules. $\rho_c = 5 \times 10^{17}kgm^{-3}$ is then given when equation 6 is no longer valid, in which the relavatisitc approximation is then used [a]. The maximum

mass obtainable due to an ideal gas of degenerate neutrons is $5.8M_s$[m] and the maximum mass due to the TOV model dependant on the equation of state is between $3M_s$ and $5M_s$ [b].

We apply the BJ EOS central density region to comply simultaneously with both limits of the EOS's in the simulation described below. Equations (4) and (5) will be used in conjunction with the differential equations in the previous section to simulate neutron stars. Both the BJ and NI equation of state assume a non-rotating neutron star.

COMPUTATIONAL METHOD

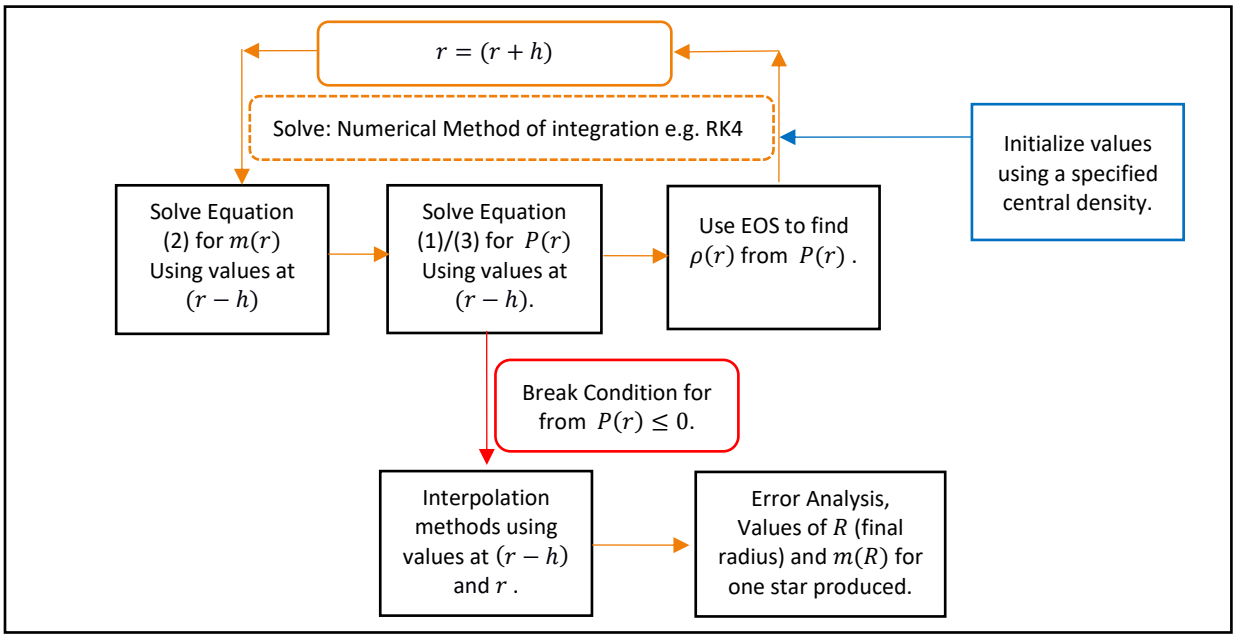

Figure 1: Computational method for a single central density.

The code for simulation was written in Python 3.5.3 using numerical integration as the base method to build neutron star from a range of initial central densities. The primary numerical integration method used was the Runge-Kutta 4th order method (RK4). Referring to Figure 1, a central density was initialised from the allowed limits. The central mass and radius were both initialized as zero [f]. A multistep numerical integration method was used until the program hit the break condition. The code then takes the last two points and interpolates using a linear fit and Newton Raphson to find the exact radius at which the pressure goes to zero. A linear fit was then applied to the respective masses and interpolation was used to find the final mass on the neutron star at the final radius.

The above method was implemented for a family of neutron stars constrained by the BJ EOS central density limitations for comparative analysis against the NI EOS.

The BJ EOS central pressure was initialized by specifying the central density and using a Newton Raphson with equation (4). The NI EOS depends on two sub EOS's as mentioned in previous sections. Therefore, when the program iterates through the numerical integration, decreasing in density until the critical density is reached (if the initial is above the critical density), the EOS then changes from equation (5.b) to (5.a) as lower density regions are reached.

Plots of final mass vs final radius, central density vs final mass and central density vs final radius were all plotted. In addition, density/matter distribution graphs were plotted to show the internal structure on the star produced by their respective EOS and gravitational model.

Furthermore, Runge Kutta 5th order (RK5) and Euler numerical integration methods were implemented. The RK5 is mathematically more accurate than RK4 but with more numerical rounding error due to extra calculations in the code. The Euler method is mathematically less accurate than the RK4, but with only a single calculation it provides the least rounding error. These two methods provide an indicative bound for our simulation result, with the RK4 chosen as the most suitable method for the primary results.

ERRORS

To calculate the errors on the mass and radius of the simulated neutron stars, two main elements of error were considered. The error in interpolation method is

$$E_{inter} = \pm(x_i - x_{i-1})^{n+1} \tag{7}$$

[g], where x_i , $x_{i-1}$are the respective points being interpolated and n is the order of polynomial, in our case this is linear and therefore $n = 1$. The error on the RK4 is calculated by simultaneously building the star with an RK4 that has a step of twice that of the step size used for the result. The equation for the RK4 error is

$$E_{RK4} = \frac{|X_{2h} - X_h|}{(2^n - 1)} \tag{8}$$

[h], where X_h is the final value of numerical integration such as the mass or radius with single step of h and X_{2h} is the RK4 double stepped final value. Both the radius and the mass had both errors for equations (6) and (7) added in quadrature for their respective values.

FICTITIOUS FORCES

The NI and BJ EOS's assume a non-rotating neutron star. To give a simple indication of what effect rotation would have on the structure of neutron stars, the pressure gradients of equations (1) and (3) were adapted to include the special relativistic centrifugal fictitious force on a shell of mass at a given radius [i].

RESULTS AND DISCUSSION

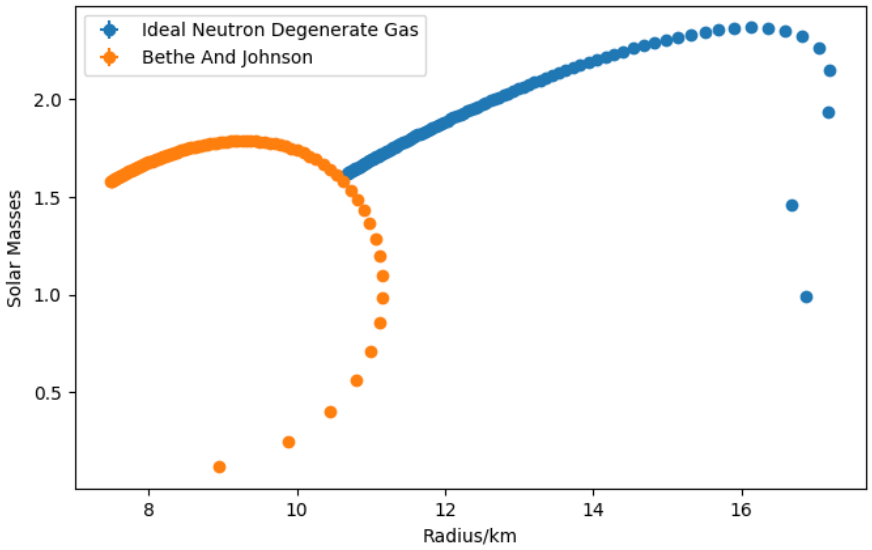

Figure 2: TOV Gravitational model, star mass against star radius displaying both EOS's from the central density limits.

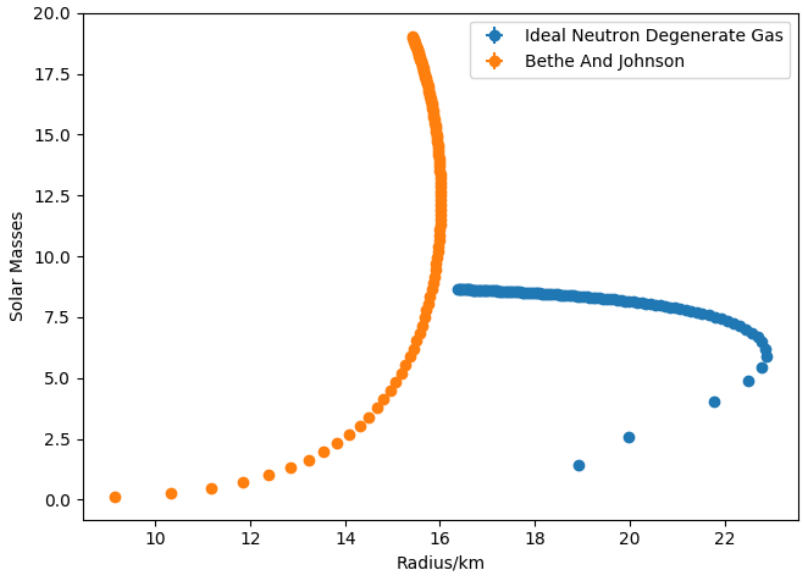

Figure 3: Newtonian Gravitational model, star mass against star radius displaying both EOS's from the central density limits.

Figures 2 and 3 compare the BJ and NI EOS's for the TOV and Newtonian model respectively. Figure 2 is under the TOV model for gravitation, the mass range for both EOS's fits limitations to the TOV model and is comparable the observed values[o]. These are masses between 1.3 to 2.5 solar masses and radii

of about 10 kilometres. Figure 3 shows that the BJ EOS under the Newtonian model exceeds the maximum mass allowable by neutron degeneracy and so is not an accurate model. The NI model under the Newtonian formalism still exceeds predicated mass by theory but still fits to a much better degree than that on the BJ EOS.

Therefore, from above we conclude the General Relativistic regime provides a more accurate model than Newtonian when compared to observation. This is as expected under the conditions of a relativistic system. We therefore provide results under the TOV model.

Our results show the maximum mass of a neutron star of the BJ EOS was found to be $(1.78840 \pm 0.00004)M_s$ with radius$(9.262 \pm 0.002)km$, the maximum radius was found to be $(11.156 \pm 0.002)km$with mass $(0.98280 \pm 0.00004)M_s$and the minimum mass is $(0.1174 \pm 0.00004)M_s$ with radius$(8.9535 \pm 0.002)km$. The maximum mass of the NI EOS was found to be $(2.36860 \pm 0.00004)M_s$ with radius $(16.125 \pm 0.002)km$, the maximum radius was found to be (17.190±0.002) km with mass (2.15130±0.00004) M_s and the minimum mass is $(0.9916 \pm 0.00004)M_s$ with radius $(16.8620 \pm 0.002)km$

The BJ and NI EOS hence fit well with current observations of neutron stars. The NI EOS fits very well with mass observations but does not with radius. This may be due to the assumption of a non-interacting neutron model or the critical density at which the relativistic NI EOS is implemented. Minimum bounds for the masses as part of our result due to TOV models are masses under the 1.4 M_s Chandrasekhar limit. We may observe neutron stars with masses slightly less than 1.4 M_s due to the star ejecting some of its own mass under gravitational collapse onto the neutron degenerate core as mentioned in theory. The lower bound approximate limitation due to stellar evolution (Chandrasekhar limit) may explain the non-unique solutions seen in Figure 3 meaning that the lower mass solutions are just a product of the mathematical model and are unphysical.

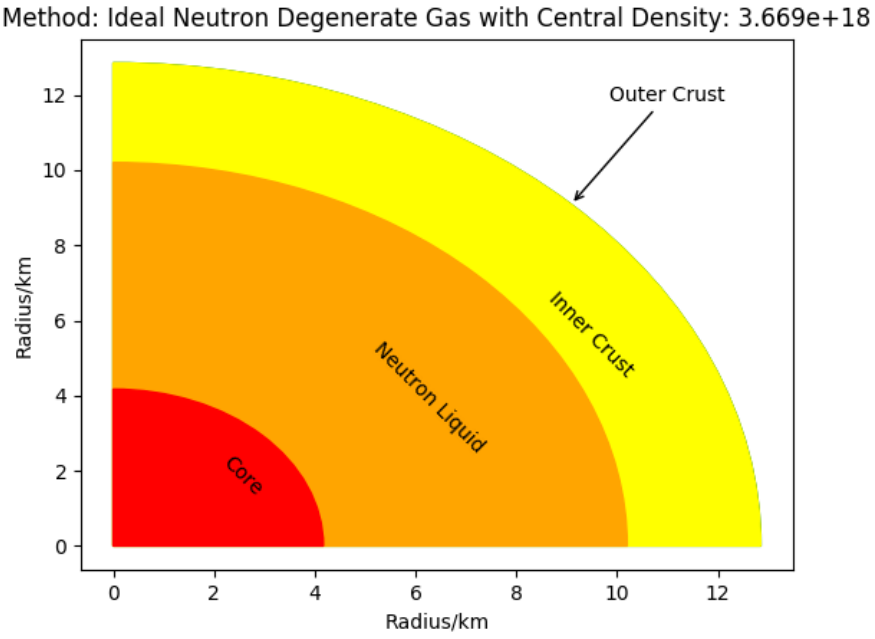

Figure 4: Density distribution model for NI EOS under the TOV model.

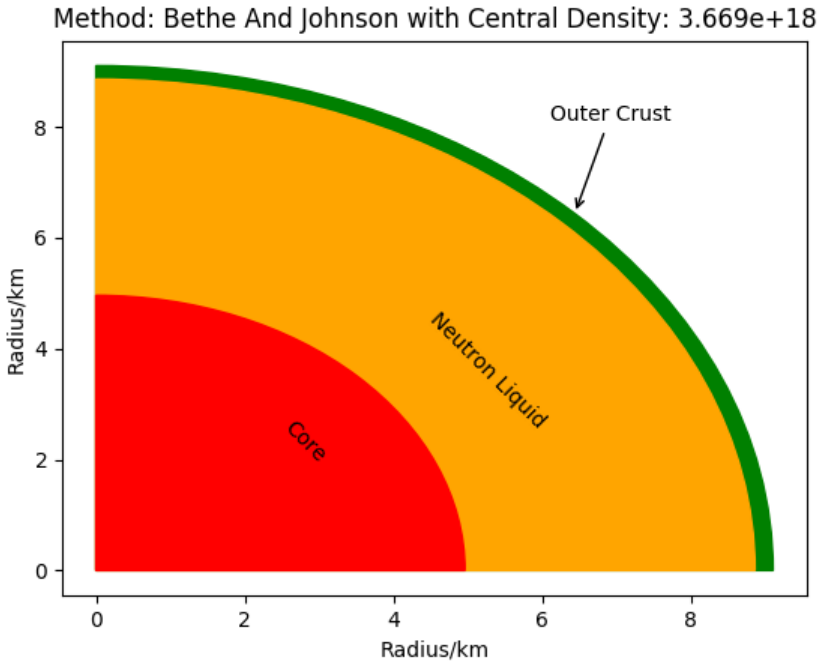

Figure 5: Density distribution model for BJ EOS under the TOV model.

Figures 4 and 5 provide an insight as to how the NI and BJ EOS's simulate the neutrons stars internal structure under the TOV model for a specified central density. The core beyond $1x10^{18}kgm^{-3}$; the BJ EOS has a slightly larger core than that of the NI EOS, this is due to the N-N interactions (and further hypothesized interactions such as pion condensation or quark matter) creating a more repulsive or soft core. As mentioned in theory at high densities interactions between particles play a much larger role in the EOS due to being over the nuclear saturation density. The neutron liquid region between $1x10^{18}kgm^{-3}$and $2.3x10^{17}kgm^{-3}$ is the point at which the EOS's begin to diverge. With the NI EOS having a much larger region than the BJ, this region is also the point at which the relativistic NI EOS is relevant due to equation 6. The inner crust corresponds the region of $2.3x10^{17}kgm^{-3}$ down to $4.3x10^{14}kgm^{-3}$where the BJ EOS has an extremely low proportion of its distribution within this region compared to the NI. The NI is most appropriate at the stage due to the lesser importance on N-N interactions when using the non-relativistic model. The outer crust is densities of less than that of the above, the BJ has a larger region than the NI EOS showing that the BJ EOS's surface is composed of a lattice structure whereas the NI EOS is almost immediately within the neutron drip region.

COMPUTATIONAL RESULTS

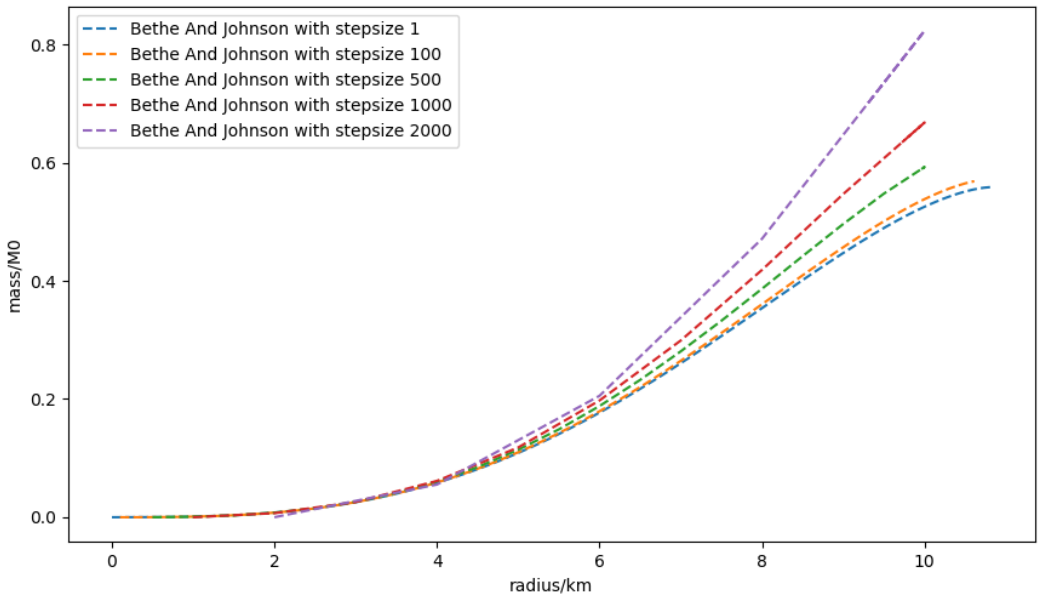

Figure 6: The effects of changing step size in the RK4.

The simulation above was calculated using step sizes of 1 meter, Figure 6 shows how an increase in step sizes creates a divergence from the true integration value. The RK4 and Euler numerical integration methods were also run for the NI and BJ EOS's under the TOV model through the entire computational method, intended to give numerical bounds to our results above. Appendix-1A shows the resulting data comparison. For such a small step size of 1-meter relative size of a neutron star the RK4 and Euler method give similar values, whereas the RK5 always produced a larger value no matter the quantity. The RK5 at this point diverges due to numerical rounding error and there shows a disadvantage to using SI units instead of unitless variables.

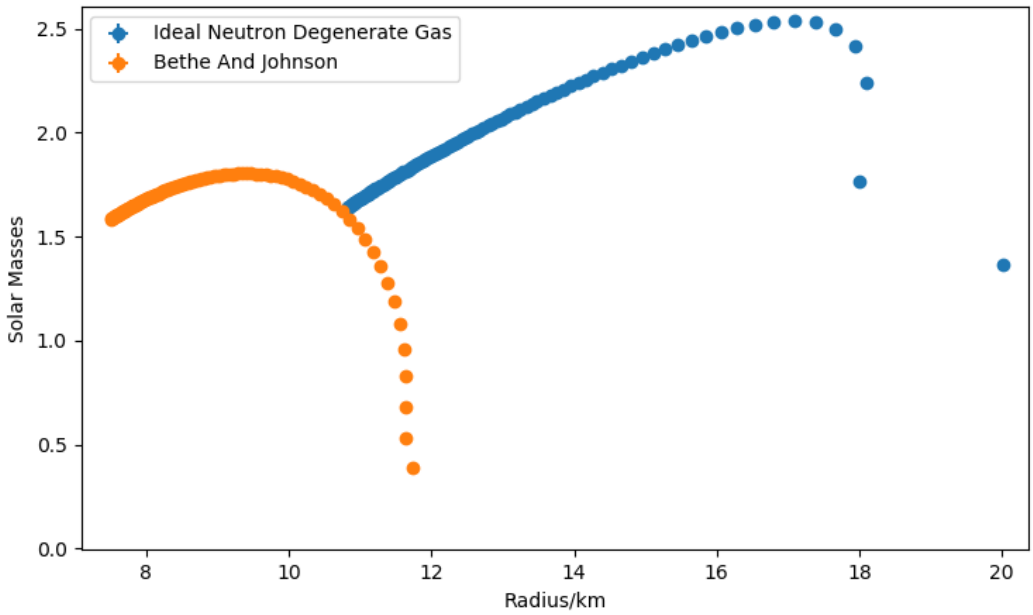

Figure 7: Rotational effects on a neutron star by modification of the pressure gradients in the TOV model.

The effects of rotation using a first order special relativistic approximation and a frequency of 641 Hz corresponding to one of the fasted observed neutron star rotations [n]. Both EOS's and the TOV were used for this exercise. The change to the maximal mass and radius increase respectively for the NI EOS was approximately 6.72% and 14.17%. The increase to the maximal mass and radius increase respectively for the BJ EOS was approximately 1.04% and 5.1%. This shows an increase although very small in comparison with the size of the star. The Newtonian model provides a similar result for rotation. More accurate calculations account for second-order Doppler boosts, the oblate spheroid shape and quadrupole moments of neutron stars [y] giving a radial increase of approximately 4% for a 1.4 $M_s$star rotation at 600Hz [y].

SUMMARY

The NI and BJ EOS's were compared across Newtonian and General relativistic regimes. The BJ EOS under the TOV gravitational model was found to be the most accurate when compared to current neutron star observations. This is due to the BJ EOS considering N-N soft core interactions unlike the NI EOS. The maximum mass of a neutron star of the BJ EOS was found to be $(1.78840 \pm 0.00004)M_s$ with radius$(9.262 \pm 0.002)km$. The density distributions for The NI and BJ EOS's were analysed and the effects of rotation were explored showing an increase in maximum radius and mass for the EOS's. Multiple methods of integration were tested to show an additional bound to our results, this showed that for a more complex integration method unitless variables should be considered to avoid rounding error.

Additional investigations aimed at giving a more complete representation of a neutron star simulation could use different EOS's within the same integration for a singular star using critical densities as bounds between them to reflect the different types of interactions at varying densities. And more appropriate EOS's may be used when considering rotation. This report aims to gives a base to such investigations.

APPENDIX - 1A

Integration Method	**RK5**	**RK4**	**Euler**
Maximum Mass (NI)	$2.6023\,M_s$	$2.3686M_s$	$2.3672\,M_s$
Maximum Mass Radius (NI)	$17.0342\ km$	$16.1247\ km$	$16.1250\ km$
Maximum Radius (NI)	$18.2221\ km$	$17.1901\ km$	$17.1945\ km$
Maximum Radius Mass (NI)	$2.3848\,M_s$	$2.1513\,M_s$	$2.1514\,M_s$
Maximum Mass (BJ)	$1.9329\,M_s$	$1.7884\,M_s$	$1.7868\,M_s$
Maximum Mass Radius (BJ)	$9.8616\ km$	$9.2616\ km$	$9.2640\ km$
Maximum Radius (BJ)	$11.8762\ km$	$11.1554\ km$	$11.1612\ km$
Maximum Radius Mass (BJ)	$1.1035\,M_s$	$0.9828\ M_s$	$0.9825\,M_s$

REFERENCES

[a] Irvine, J. (1978). *Neutron stars*. Oxford: Clarendon Press, pp.115-131.

[b] Shapiro, S. and Teukolsky, S. (1983). *Black holes, white dwarfs, and neutron stars*. New York: Wiley, pp.188-294.

[c] Phillips, A. (2013). The Physics of Stars. Hoboken: Wiley, pp.30-31.

[d] Bethe, H. and Johnson, M. (1974). *Dense baryon matter calculations with realistic potentials*. Nuclear Physics A, 230(1), pp.1-58.

[e] A.S.Chai. *Error estimate of a fourth-order Runge-Kutta method with only one initial derivative evaluation*. Hybrid Computer Laboratory, University of Wisconsin Madison.

[f] M.Hjorth-Jensen; Computational Physics; *http://folk.uio.no/mhjensen/computationalphysics.pdf* (2006) p289-293

[g] *Polynomial Interpolation: error analysis*. Available from: https://www.math.uh.edu/~jingqiu/math4364/interp_error.pdf [Accessed 21 March 2018].

[h] Error estimate of a fourth-order Runge-Kutta method with only one initial derivative evaluation https://www.computer.org/csdl/proceedings/afips/1968/5071/00/50710467.pdf [Accessed 21 March 2018].

[i] Jonsson, R. (2006). An intuitive approach to inertial forces and the centrifugal force paradox in general relativity. American Journal of Physics, 74(10), pp.905-916.

[j] Jolien Creighton (2012). *Relativistic Stars*. University of Wisconsin–Milwaukee.

[k] Hook, J. and Hall, H. (2013). Solid state physics. Hoboken: Wiley, pp.52-82.

[n] Chakrabarty, D., Morgan, E., Muno, M., Galloway, D., Wijnands, R., van der Klis, M. and Markwardt, C. (2003). *Nuclear-powered millisecond pulsars and the maximum spin frequency of neutron stars*. Nature, 424(6944), pp.42-44.

[h] Oppenheimer, J. and Volkoff, G. (1939). On Massive Neutron Cores. Physical Review, 55(4), pp.374-381.

[m] Phillips, A. (2013). The Physics of Stars. Hoboken: Wiley, pp.171-204.

[o] https://www.nasa.gov/mission_pages/GLAST/science/neutron_stars.html

[p] Paweł Haensel, Alexander Y. Potekhin and Dmitry G. Yakovlev. (2007). Neutron Stars, pp.12. Springer.

[y] Bauböck, M., Özel, F., Psaltis, D. and Morsink, S. (2015). ROTATIONAL CORRECTIONS TO NEUTRON-STAR RADIUS MEASUREMENTS FROM THERMAL SPECTRA. The Astrophysical Journal, 799(1), p.22.

[q] Irvine, J. (1978). *Neutron stars*. Oxford: Clarendon Press, pp.1-5.

[r] Phillips, A. (2013). The Physics of Stars. Hoboken: Wiley, pp.5-10.